Am J Physiol Heart Circ Physiol 290: H732–H740, 2006.
First published September 30, 2005; doi:10.1152/ajpheart.00747.2005.

Alterations in blood-brain barrier ICAM-1 expression and brain microglial activation after λ-carrageenan-induced inflammatory pain

J. D. Huber,[1] C. R. Campos,[2] K. S. Mark,[3] and T. P. Davis[2]

[1]*Department of Basic Pharmaceutical Sciences, West Virginia University, Morgantown, West Virginia;*
[2]*Department of Medical Pharmacology, University of Arizona, Tucson, Arizona; and*
[3]*Department of Pharmacology, University of Missouri-Kansas City, Kansas City, Missouri*

Submitted 14 July 2005; accepted in final form 25 September 2005

Huber, J. D., C. R. Campos, K. S. Mark, and T. P. Davis. Alterations in blood-brain barrier ICAM-1 expression and brain microglial activation after λ-carrageenan-induced inflammatory pain. *Am J Physiol Heart Circ Physiol* 290: H732–H740, 2006. First published September 30, 2005; doi:10.1152/ajpheart.00747.2005.—Previous studies showed that peripheral inflammatory pain increased blood-brain barrier (BBB) permeability and altered tight junction protein expression and the delivery of opioid analgesics to the brain. What remains unknown is which pathways and mediators during peripheral inflammation affect BBB function and structure. The current study investigated effects of λ-carrageenan-induced inflammatory pain (CIP) on BBB expression of ICAM-1. We also examined the systemic contribution of a number of proinflammatory cytokines and microglial activation in the brain to elucidate pathways involved in BBB disruption during CIP. We investigated ICAM-1 RNA and protein expression levels in isolated rat brain microvessels after CIP using RT-PCR and Western blot analyses, screened inflammatory cytokines during the time course of inflammation, assessed white blood cell counts, and probed for BBB and central nervous system stimulation and leukocyte transmigration using immunohistochemistry and flow cytometry. Results showed an early increase in ICAM-1 RNA and protein expression after CIP with no change in circulating levels of several proinflammatory cytokines. Changes in ICAM-1 protein expression were noted at 48 h. Immunohistochemistry showed that the induction of ICAM-1 was region specific with increased expression noted in the thalamus and frontal and parietal cortices, which directly correlated with increased expression of activated microglia. The findings of the present study were that CIP induces increased ICAM-1 mRNA and protein expression at the BBB and that systemic proinflammatory mediators play no apparent role in the early response (1–6 h); however, brain region-specific increases in microglial activation suggest a potential for a central-mediated response.

neurovascular unit; adhesion molecule; intercellular adhesion molecule-1; proinflammatory mediators; leucocyte transmigration

THE CENTRAL NERVOUS SYSTEM (CNS) has long been characterized as an immune-privileged site due to the lack of lymphatic tissue and strict regulation of the parenchymal microenvironment by the blood-brain barrier (BBB). However, the brain is now recognized as having its own innate immune system and immune effector cells (microglia) that enable the CNS to rapidly respond to injury or disease. Several CNS-associated diseases have been characterized by cerebral inflammatory processes resulting from exogenous antigens and decreased peripheral tolerance to self-antigens that alter BBB physiological function, leading to disruptions in homeostasis, neuronal function, and delivery of therapeutic agents (10, 21, 30, 32, 43). A growing body of evidence details the pivotal role that cerebral inflammation plays in neuronal injury and central-mediated inflammatory processes, including localized activation of resident cells (i.e., microglial, astrocytes), recruitment of leukocytes into the CNS, and release of proinflammatory cytokines (3, 8, 39, 40).

ICAM-1 plays an important role in immune-mediated cell-cell adhesive interactions (41) and intracellular signal transduction pathways through outside-in signaling events (23, 29). ICAM-1 expression in cerebral microvessels, under basal conditions, is low (45); however, ICAM-1 is markedly increased on the luminal surface of endothelial cells in the presence of proinflammatory mediators, such as TNF-α, IL-1β, IL-4, and IFN-γ, primarily due to de novo mRNA transcription and translation (15, 31, 46). Once stimulated, the endothelial cell undergoes a number of morphological changes, including increased surface expression of adhesion molecules, cytoskeletal reorganization, and activation of signaling pathways (5, 17, 37). A strong and repeatable correlation between induction of ICAM-1 and increased BBB permeability has been shown in a number of pathologies characterized by acute inflammation, including atherosclerosis, ischemia, human immunodeficiency virus encephalitis, and autoimmune disorders (4, 19, 38, 47). Furthermore, loss of endothelial cell, tight junction proteins, occludin, and zonula occludens-1 was observed in cerebral vascular endothelium during neutrophil-induced BBB breakdown (1). All of these findings suggest that upregulation in ICAM-1 expression may play a primary role in regulating BBB function and structure.

An association between increased ICAM-1 expression and activated microglia has been shown during central-mediated cerebral inflammation (6, 24, 25). Microglial cells are ubiquitously located throughout the brain parenchyma with many situated near blood vessels, with microglial processes having direct contact with the basal lamina of cerebral microvessels (27). The functional role of the physical interaction between these juxtavascular microglia and cerebral microvessels is still unknown; however, juxtavascular microglial cells have been reported to exhibit a more robust response than nonjuxtavascular microglia on activation (12). Recent studies in a number of different pain models, including acute and chronic inflammation and neuropathic, have shown spatial localization of activated microglia in the spinal cords of rats (13, 28) after induction of pain with a noxious stimuli. What is currently

Address for reprint requests and other correspondence: T. P. Davis, Dept. of Medical Pharmacology, Univ. of Arizona, Tucson, AZ 85721 (e-mail: davistp@u.arizona.edu).

The costs of publication of this article were defrayed in part by the payment of page charges. The article must therefore be hereby marked "*advertisement*" in accordance with 18 U.S.C. Section 1734 solely to indicate this fact.

unknown is whether peripheral inflammation activates microglial cells in the brain and what effect activation may have on the structure and function of the BBB.

Recent studies in our laboratory have shown that peripheral, localized inflammatory pain elicited functional and structural alterations at the BBB, including a biphasic increase in paracellular permeability, changes in tight junction protein expression (17, 18), and altered delivery of codeine into the CNS (16). Of importance in our findings was that changes in permeability and alterations in protein expression occurred at an early (1–6 h) and delayed (48 h) phase after λ-carrageenan-induced inflammatory pain (CIP). The similarities in our findings and those investigating changes of the BBB during CNS-based pathologies are intriguing.

The first objective of this study was to determine the effect of CIP on the cerebral microvessel expression of ICAM-1 from 0–72 h. The second objective was to examine potential mediators involved in the structural and functional perturbations of the BBB observed at 1–6 and 48 h after CIP. Specifically, we examined the systemic contribution of a number of proinflammatory cytokines and the activation of microglial cells in the brain to elucidate possible pathways involved in our previously described BBB disruption during CIP.

MATERIALS AND METHODS

Animals and treatments. Female Sprague-Dawley rats (Harlan, Indianapolis, IN) weighing 225–249 g were housed under standard 12:12-h light-dark conditions and received food ad libitum. A total of 138 rats were used in this study. All protocols involving animals were approved by the University of Arizona Institutional Animal Care and Use Committee and abide by National Institutes of Health guidelines. Rats were anesthetized (60 mg/kg ip pentobarbital sodium) and injected (100 μl sc) with 3% λ-carrageenan into the plantar surface of the right hind paw. Previous studies have shown no difference in BBB structure and function between nontreated and saline-injected rats, regardless of time after injection; therefore, control animals consisted of animals injected (100 μl sc) into the right hind paw with 0.9% saline and immediately euthanized (0 h).

Microvessel isolation. At 0, 0.25, 0.50, 0.75, 1, 3, 6, 12, 24, 48, and 72 h after CIP, the rats were anesthetized with pentobarbital sodium (60 mg/kg ip), decapitated, and the brains removed. Meninges and choroid plexuses were excised and cerebral hemispheres homogenized in 4 ml of microvessel isolation buffer [103 mM NaCl, 4.7 mM KCl, 2.5 mM KH_2PO_4, 1.2 mM $MgSO_4$, 15 mM HEPES, 2.5 mM $NaHCO_3$, 10 mM D-glucose, 1 mM sodium pyruvate, and 10 g/l dextran (mol wt 64,000); pH 7.4] with a Complete-mini protease inhibitor tablet (1 tablet per 10 ml; Roche, Indianapolis, IN). Four milliliters of ice-cold 26% dextran were added to the homogenate and vortexed. Homogenates were centrifuged at 5,600 *g* for 10 min, and the supernatant was aspirated. Pellets were resuspended in 10 ml of microvessel isolation buffer and passed through a 70-μm filter (Becton Dickinson, Franklin, NJ). Filtered homogenates were pelleted by centrifugation at 3,000 *g*.

RNA extraction and expression of ICAM-1. At 0, 0.25, 0.50, 0.75, 1, 3, 6, 12, 24, 48, and 72 h after CIP, total RNA was extracted from isolated cerebral microvessels ($n = 3$ per time point) with the use of TriReagent (Sigma). RNA quality was verified by ethidium bromide staining of ribosomal RNA bands (28S and 18S) on a 1.5% agarose-20% formaldehyde gel. Before RT-PCR, total RNA was pretreated with DNase I (type II, Sigma), and quantified by spectrophotometry (A260/A280 ratio > 1.80).

With the use of RT-PCR, 1 μg of total RNA at each time point was amplified by using a SuperScript One-Step PCR kit (Life Technologies, Rockville, MD) with an initial denaturation step (94°C for 4 min), 35 cycles (94°C for 30 s, 50°C for 30 s, and 72°C for 30 s), and a final extension step (72°C for 4 min) with the use of a GeneAmp 2100 (PerkinElmer, Torrance, CA). Primers for long terminal repeats of ICAM-1 5′-AGCATTTACCCCTCACCCAC-3′ (forward) and 5′-CATTTTCTCCCAGGCATTCTC-3′ (reverse) and β-actin (internal control) 5′-TACAACCTCCTTGCAGCTCC-3′ (forward) and 5′-GGATCTTCATGAGTAGTCTGT-3′ (reverse) were purchased from Sigma-Genosys (St. Louis, MO). The cDNA products were run on a 2% agarose gel with ethidium bromide at 125 V for 40 min, illuminated under ultraviolet light, and photodocumented.

Protein extraction, immunoprecipitation, and Western blot analysis of ICAM-1. At 0, 0.25, 0.50, 0.75, 1, 3, 6, 12, 24, 48, and 72 h after CIP, crude protein was extracted from isolated cerebral microvessels ($n = 4$/time point) with the use of 6 M urea lysis buffer (6 M urea, 0.1% Triton X-100, 10 mM Tris base, 1 mM dithiothreitol, 5 mM $MgCl_2$, 5 mM EGTA, and 150 mM NaCl; pH 8.0) with protease inhibitor tablet (Roche). Protein concentrations were determined by bicinchoninic acid protein assay (Pierce, Rockford, IL) with the use of bovine serum albumin as a standard.

Immunoprecipitation studies were performed to determine ICAM-1 expression in isolated microvessel homogenates. In brief, 100 μg of total protein were diluted 10-fold with lysis buffer without urea, combined with 5 μg anti-ICAM-1 (Zymed, South San Francisco, CA), and incubated overnight at 4°C. The next day, 50 μl of rec-protein G Sepharose beads (Zymed) were added. Samples were incubated for 6 h at 4°C, pelleted, and washed twice with 1 M urea lysis buffer and once with lysis buffer without urea. Samples were resuspended in 2× Laemmli sample buffer (1 M Tris·HCl, 4% wt/vol SDS, 30% glycerol, 1% β-mercaptoethanol, and 0.05% bromophenol blue; pH 6.8) and heated to 96°C for 10 min before electrophoresis.

ICAM-1 immunoprecipitants were resolved on 4–12% Tris-glycine gels (Novex, San Diego, CA) for 90 min at 125 V and transferred to polyvinylidene difluoride membranes for 30 min at 240 mA. Polyvinylidene difluoride membranes were blocked in Tris-buffered saline (141 mM NaCl, 10 mM Tris base, and 0.1% Tween-20; pH 7.4) with 5% nonfat milk for 4 h. Blots were incubated with anti-rabbit IgG (Sigma) for 1 h. Membranes were washed four times with 5% nonfat milk for 10 min. Blots were developed by using enhanced chemiluminescence (ECL+; Amersham Life Science Products, Springfield, IL) and analyzed with Scion Image software (Scion, Frederick, MD).

Immunocytochemistry for ICAM-1, polymorphonuclear neutrophils, and microglia. At 0, 3, 48, and 72 h after CIP, the rats ($n = 3$/time point) were anesthetized with pentobarbital sodium (60 mg/kg ip) and underwent transcardiac perfusion with 100 ml of 0.1 M PBS (pH 7.4) followed by 100 ml of 4% paraformaldehyde-PBS. The brains were postfixed overnight at 4°C in 4% paraformaldehyde-PBS, placed in 20% sucrose-PBS for 24 h, and then 30% sucrose-PBS for 24 h. The brains were embedded in Tissue-Tec optimal cutting temperature compound (Miles, Elkhart, IN), sliced into 20-μm sections, mounted on Super Frost Plus slides (Fisher Scientific, Pittsburgh, PA), and frozen at −80°C. The brain slices in this study were analogous to plate 29 from *The Rat Brain in Stereotaxic Coordinates* (35). On use, the slides were thawed, washed in PBS for 10 min, and treated with 0.3% H_2O_2-30% methanol in PBS for 30 min to suppress endogenous peroxidases.

Nonspecific binding was blocked by using 10% goat or horse serum in PBS for 30 min at room temperature. Sections were incubated in rabbit anti-human CD54 (ICAM-1; 1:1,000; Zymed), rabbit anti-human MPO [polymorphonuclear neutrophils (PMNs); 1:250; Dako, Carpinteria, CA] or mouse anti-rat OX42 (microglia/macrophage; 1:100, Serotec, Oxford, UK) overnight at 4°C. The brain sections were washed with PBS three times for 10 min at room temperature and incubated with biotinylated goat anti-rabbit or horse anti-mouse IgG (Vector Laboratories, Burlingame, CA) for 60 min at room temperature followed by an avidin-biotin complex process (Vector Laboratories). Finally, the brain sections were exposed to stable 3,3′-diaminobenzidine tetrahydrochloride (DAB) and enhanced

(DAB enhancer, Zymed) if necessary. Anti-vimentin (1:1,000; Zymed) was used as a positive control. Negative control experiments were performed by using biotinylated anti-rabbit and anti-mouse IgG instead of primary antibody. In addition, selected brain slices were processed with no primary or secondary antibody. Selected brain sections were counterstained with hematoxylin. All incubations were carried out in a humidified chamber.

White blood cell and cytokine profile in the systemic circulation. At 0, 1, 3, 6, 12, 24, 48, and 72 h after CIP, blood was drawn (12–15 ml) from the descending aorta of rats ($n = 6$/time point) into EDTA-coated tubes. An aliquot of blood was taken for blood cell counts with the use of an automated cell counter (model 9018 CP; Serono Diagnostics, Allentown, PA). Leukocyte differential counts were verified manually on Wright-stained blood smears. Red blood cell counts, white blood cell (WBC) counts, hematocrit, and WBC differential were all recorded. Immature and small leukocytes were grouped together as "undifferentiated." Two 1-ml aliquots were taken for flow cytometric analyses. The remaining blood was centrifuged at 800 *g* for 10 min. Supernatant (plasma) was collected in 200-μl aliquots and frozen at −80°C until needed for determination of cytokine levels in the systemic circulation.

Inflammatory cytokine determination in systemic circulation. TNF-α, IL-1β, IL-6, IL-10, and IFN-γ were evaluated by colorimetric assay with the use of Quantikine HS ELISA kits (purchased from R&D Systems, Minneapolis, MN) according to the manufacturer's instructions. Briefly, samples ($n = 6$/time point) and standards were incubated for 2 h in a diluent solution containing an immobilized capture antibody specific to the analyte of interest. After incubation, wells were rinsed and a biotin-conjugated secondary epitope was added to each well to form an analyte-antibody conjugate. After another series of washes, a streptavidin-horseradish peroxidase solution was added to each well and biotin-conjugated antibodies were formed. Hydrogen peroxide-tetrabenzidine solution (50 μl) was added and incubated for 30 min, and 50 μl of sulfuric acid were then added to stop reaction. Determination of optical density was determined by using a microplate reader set to 490 nm with a 650-nm correction within 30 min of the stop reaction. Cytokine concentrations were calculated from a curve generated from the absorbance of the standards.

Brain removal and isolation of immunocompetent brain cells. At 0, 3, 48, and 72 h after CIP, the rats ($n = 3$/time point) were anesthetized with pentobarbital sodium (60 mg/kg) and perfused with 0.9% saline (containing 2 U/ml heparin) to remove blood from the brain vasculature. The method used for preparation of a microglia-enriched isolate was modified from a previously published method (2) to include an enzymatic dissociation step. The brain was removed and the meninges and choroid plexuses were excised. Olfactory bulbs and cerebellum were excised, and the whole brain was mechanically dissociated and placed in 2 ml of dissociation buffer [Hank's balanced salt solution (HBSS) with 20 U/ml collagenase II and 25 U/ml DNase I] at 37°C for 45 min. After dissociation, cells were washed twice with HBSS, passed through a 40-μm nylon cell strainer, centrifuged at 400 *g* for 10 min, resuspended in a final volume of 4 ml of 30% Percoll (Amersham Pharmacia Biotech, Springfield, IL), and overlaid on top of a gradient containing 3.5 ml of 37% Percoll and 3.5 ml of 70% Percoll. The gradient was centrifuged at 500 *g* for 20 min at room temperature. Cells were collected from the 37–70% interface (~5 ml) and washed once with HBSS containing 10% fetal bovine serum.

Flow cytometric and immunophenotypic analysis. Morphological analysis was performed by using peripheral blood in EDTA and isolated microglia. Two hundred microliters of blood were incubated in the dark with 10 μl of anti-CD3-PE (nonspecific T-cell antigen; Pharmingen, San Diego, CA), CD4-FITC (coreceptor for major histocompatibility complex class II molecules; Pharmingen) and anti-CD8-Cy5 (coreceptor of major histocompatibility complex class I molecules; Pharmingen) or anti-CD45-Cy5 (leukocyte common antigen; Pharmingen) and anti-CD18-PE [lymphocyte function-associated antigen 1 (LFA-1); Serotec, Raleigh, NC] for 20 min at room temperature. After conjugation, red blood cells were lysed by incubating in FACS lysing solution (Becton Dickinson, San Jose, CA) for 15 min at room temperature and then centrifuged at 200 *g* to pellet the WBC. WBC pellets were washed in FACSflow solution (Becton Dickinson). In addition, 200 μl of isolated microglia were incubated in the dark with 10 μl of anti-CD45, anti-CD11b/c-FITC (α_M-integrin; Serotec), and anti-CD54-PE (ICAM-1, Serotec) for 20 min at room temperature. After conjugation, microglial isolates were centrifuged at 500 *g* for 5 min, washed once, and resuspended in FACSflow solution (Becton Dickinson). In blood samples, analysis was performed by using appropriate gates to enumerate total lymphocytes ($CD3^{high}$) and leukocytes ($CD45^{high}$). $CD3^{high}$ cells were gated for expression of $CD4^{high}$ and $CD8^{high}$. $CD45^{high}$ cells were gated for expression of $CD18^{high}$. Microglial isolates were gated for cells ($CD45^{low}$/CD11b/c^{high}) to determine expression of $CD54^{high}$. Three-color flow cytometry was performed by using FACScan flow cytometer with a 15-mW argon laser (excitation at 488 nm) (Becton Dickinson). Analysis of captured cell events from each sample was accomplished with the use of CellQuest software (Becton Dickinson).

Statistical analyses. Data are expressed as means ± SE. Statistical difference between time points compared with control (0 h) was determined by using one-way ANOVA followed by Dunnett's post hoc test. Statistical significance was set at $P < 0.05$.

RESULTS

RT-PCR of ICAM-1. Amplification of total RNA from isolated microvessels by RT-PCR produced a 768-bp ICAM-1 cDNA fragment at 0 (control), 0.25, 0.50, 0.75, and 24 h postinduction of inflammatory pain (Fig. 1). Control (0 h) showed a basal level of ICAM-1 mRNA. The remaining time points indicate increased (although not quantitatively) mRNA expression immediately after treatment (0.25, 0.50, and 0.75 h) and at 24 h. β-Actin was used as an internal control.

Western blot analysis of ICAM-1 expression in rat brain microvessels. Figure 2 depicts Western blot analyses of isolated cerebral microvessels after CIP from 0 to 72 h. ICAM-1 was immunoprecipitated from total crude protein. ICAM-1 protein expression was significantly increased at 1, 3, 6, 12, 24, and 48 h postinjection (264 ± 17, 317 ± 26, 274 ± 29, 169 ± 12, 153 ± 15, and 176 ± 11%, respectively). All values were normalized as a relative percentage of control.

Immunohistochemistry for ICAM-1 expression. Few, if any, ICAM-1 immunoreactive areas were observed in the brain slices of control (0 h) rats (Fig. 3). ICAM-1 immunopositive staining was observed at 3 h in the thalamus and parietal cortex (Fig. 3) and to a lesser extent in the frontal cortex (Fig. 3). ICAM-1 immunoreactivity was not observed in the striatal or hippocampal regions at 3 h. ICAM-1 immunoreactivity was

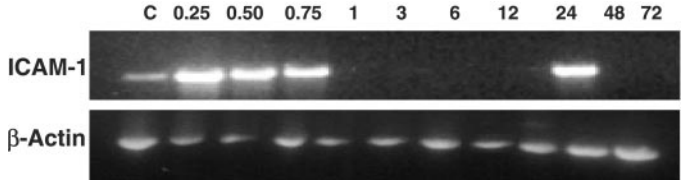

Fig. 1. Amplification of total RNA from isolated microvessels by RT-PCR produced a 768-bp ICAM-1 cDNA fragment at 0 (control), 0.25, 0.50, 0.75, and 24 h postinduction of inflammatory pain. Control (0 h) showed a basal level of ICAM-1 mRNA. Remaining time points indicate an increase (although not quantitatively) in mRNA expression immediately after treatment (0.25, 0.50, and 0.75 h) and at 24 h. β-Actin was used as an internal control. ($n = 3$ per time point).

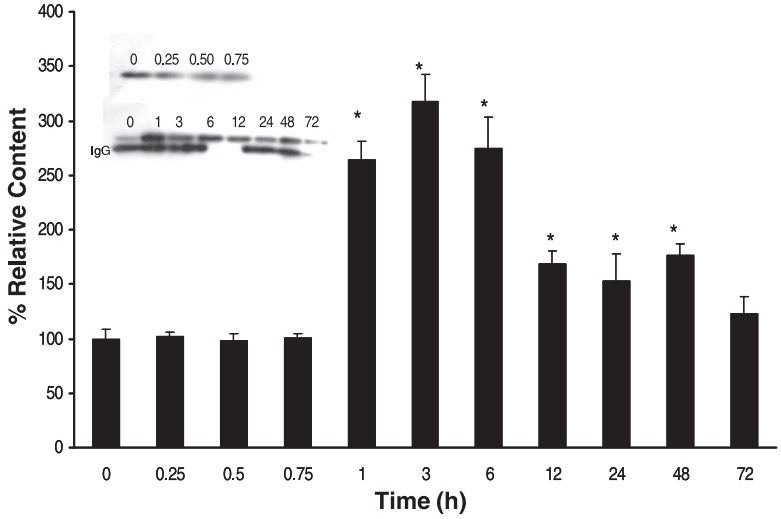

Fig. 2. Western blot analyses of isolated cerebral microvessels after λ-carrageenan-induced inflammatory pain (CIP) from 0–72 h. ICAM-1 was immunoprecipitated from total crude protein. ICAM-1 protein expression was significantly increased at 1, 3, 6, 12, 24, and 48 h postinjection (264 ± 17, 317 ± 26, 274 ± 29, 169 ± 12, 153 ± 15, and 176 ± 11%, respectively). All values are normalized as a relative percentage of control. *Insets*: representative Western blots of immunoprecipitated ICAM-1. Each bar represents means ± SE (n = 4/time point). *Significant difference from control ($P < 0.05$).

still detected at 48 and 72 h after inflammatory pain induction. At 48 h, immunostaining was observed in the parietal and frontal cortices and the thalamus. At 72 h, areas of ICAM-1 immunoreactivity were markedly decreased, especially in the thalamic region, and appeared to be localized in patches rather than diffusely spread in the cortical regions as observed at 3 and 48 h.

Immunohistochemistry for microglial (OX42) activation. Figure 4 depicts resting microglia in the parietal and temporal cortices and the thalamic region in control (0 h) brain slices. OX42 immunoreactivity was strongly expressed at 3 and 48 h as seen by activated microglia (OX 42) in the frontal and parietal cortices and thalamic region after CIP. Activated microglial cells were noted by their stout, dense

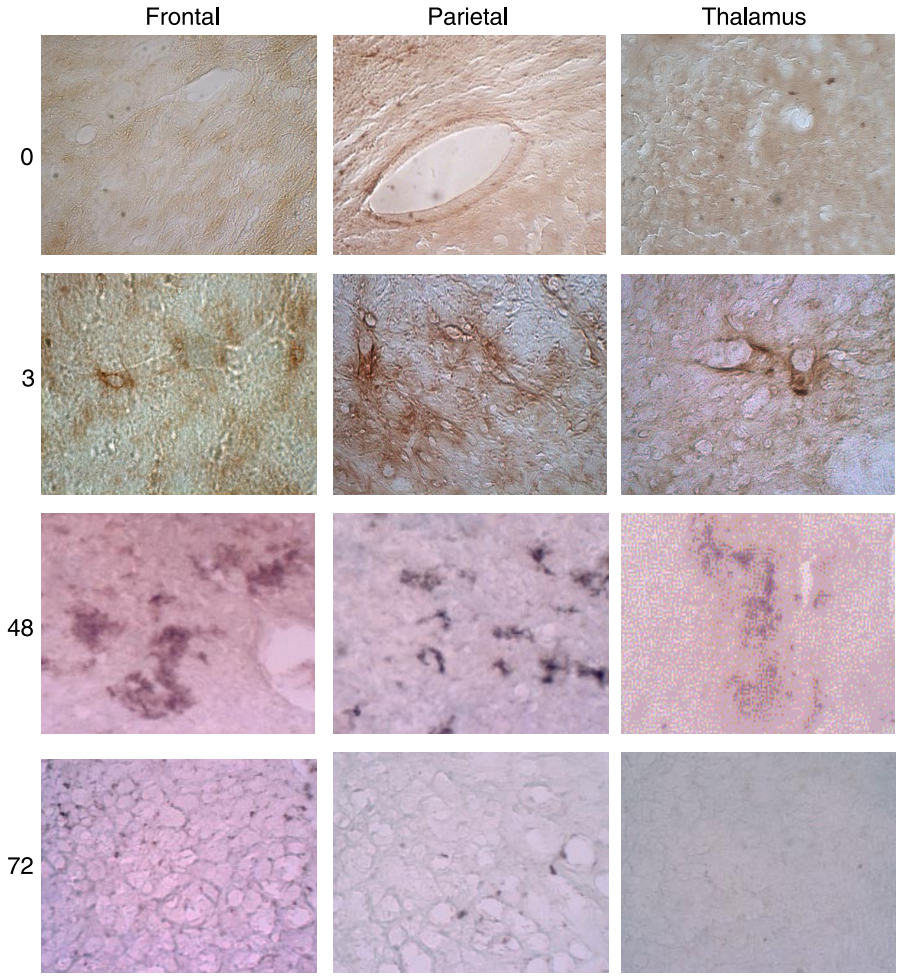

Fig. 3. ICAM-1 immunohistochemistry of brain slices of the frontal and parietal cortices and thalamic region after CIP. Results indicate no immunoreactivity in hippocampal and striatal regions. ICAM-1 immunoreactivity was observed at 3 h in frontal, parietal, and thalamic areas, especially around capillaries and postcapillary venules. ICAM-1 immunoreactivity was also observed at 48 h, with intense staining in frontal and parietal cortices and to a lesser extent in the thalamic region. Unlike at 3 h, at 48 h, staining appeared to not be localized around blood vessels but rather diffusely scattered. At 72 h, ICAM-1 immunoreactivity was diminished in all brain regions (n = 3/time point). Positive (vimentin immunoreactive) and negative (anti-IgG) controls were routinely performed to ensure consistency.

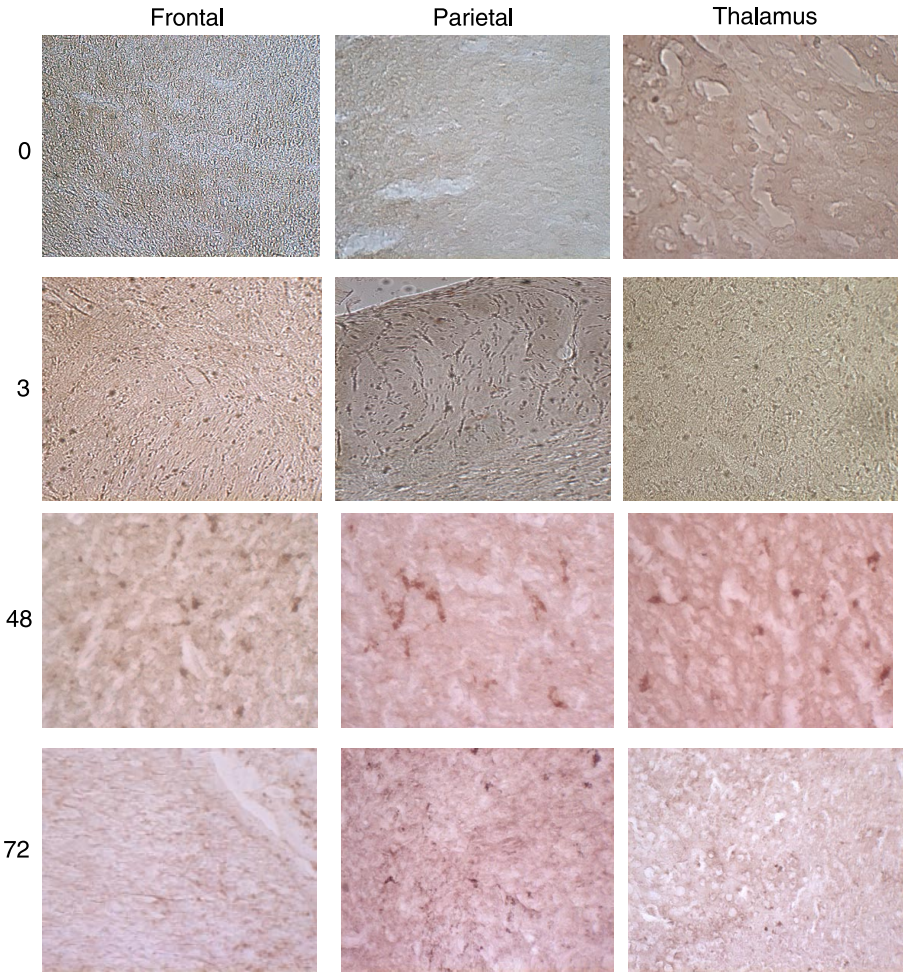

Fig. 4. Activated microglia (OX42) immunohistochemistry of brain slices of the frontal and parietal cortices and thalamic region after CIP. OX42 immunoreactivity was strongly expressed at 3 and 48 h. Activated microglial cells were noted by their stout, dense appearance with stellate projections. At 72 h, OX42 immunoreactivity was decreased compared with 3 and 48 h, with immunoreactivity primarily in the parietal cortex and to a lesser extent in the frontal cortex (n = 3/time point). Positive (vimentin immunoreactive) and negative (anti-IgG) controls were routinely performed to ensure consistency.

appearance with stellate projections. At 72 h, OX42 immunoreactivity was decreased compared with 3 and 48 h, with immunoreactivity primarily in the parietal cortex and to a lesser extent in the frontal cortex. Positive (vimentin immunoreactive) and negative (anti-IgG) controls were routinely performed to ensure consistency. No increase in OX42 reactive macrophages was observed at any time point compared with control (0 h).

Immunohistochemistry of infiltration of PMNs and macrophages. MPO immunoreactive cells (PMNs) were observed at 48 and 72 h in the thalamus and frontal and parietal cortices (Fig. 5). Figure 5 shows that most of the infiltration was localized near or adjacent to cerebral vessels. Hematoxylin counterstaining confirmed the presence of PMNs within the brain parenchyma (data not shown). No increase in OX42 reactive macrophages was observed at any time point compared with control (0 h).

Whole blood cell profile. Table 1 depicts whole blood profile for control and CIP rats (0–72 h). Results indicate no difference ($P > 0.05$) in total WBC counts at any time point when compared with control (0 h). No statistical difference ($P > 0.05$) in percentage of PMNs was observed; however, the percentage of lymphocytes as a total of WBC was significantly decreased ($P < 0.05$) at 48 and 72 h compared with control (0 h) to below levels considered normal for Sprague-Dawley rats (Taconic, Germantown, NY). In addition, the percentage of undifferentiated WBC was significantly increased ($P < 0.05$) over control (0 h) at 48 and 72 h.

Inflammatory cytokine determination in systemic circulation. With the use of ELISA, determination of cytokines (TNF-α, IL-1β, and IL-6) showed no significant change ($P > 0.05$) in plasma concentrations at any time point compared with control (0 h) (Fig. 6). Basal concentrations for these circulating cytokines fell within previously reported values (8). At 6 h, we observed a significant ($P < 0.05$) fivefold increase in IL-10 serum concentration. At 48 h, we showed a significant ($P < 0.05$) twofold increase in IFN-γ that remained constant out to 72 h and a significant ($P < 0.05$) threefold increase in IL-1β serum concentration at 72 h.

Immunophenotypic marker analysis. Figure 7, *A* and *B*, illustrates flow cytometric analyses of blood and microglial isolates. No statistical difference ($P > 0.05$) was seen in the CD4/CD8 lymphocyte ratio at any time point compared with control (0 h) (data not shown). Gating for $CD45^{high}$ cells (leukocytes) showed a significant increase ($P < 0.05$) in $CD18^{high}$ (LFA-1) expression at 48 h compared with control (0 h) (Fig. 7*A*). Gating for $CD45^{low}$/CD 11b/c^{high} cells in microglial isolates showed a significant increase in $CD54^{high}$ (ICAM-1) expression at 3 and 48 h compared with control (0 h) (Fig. 7*B*).

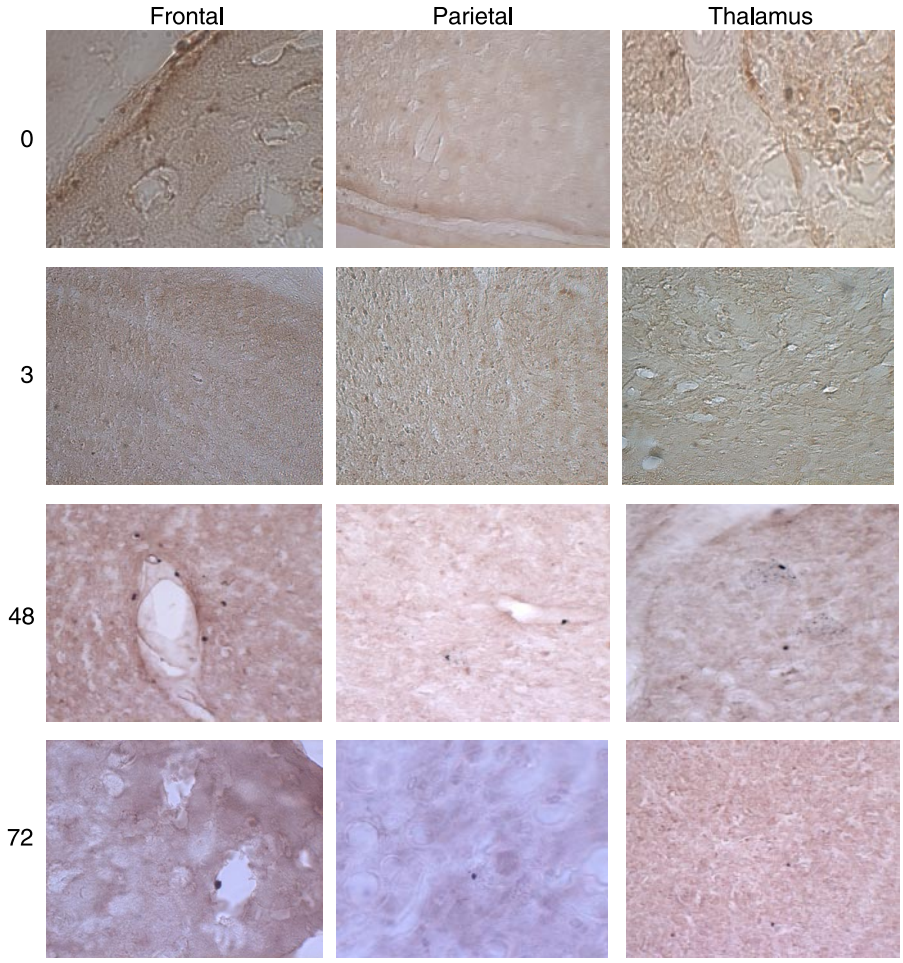

Fig. 5. MPO [polymorphonuclear neutrophils (PMNs)] immunohistochemistry of brain slices of the frontal and parietal cortices and thalamic region after CIP. No MPO immunoreactivity was noted in any brain region examined at 0 and 3 h. At 48 and 72 h, PMN immunoreactivity was observed in frontal and parietal cortices and thalamus, mostly in areas around blood vessels. PMN infiltration was confirmed by using hemotoxlin-stained slides (not shown). Positive (vimentin immunoreactive) and negative (anti-IgG) controls were routinely performed to ensure consistency (n = 3/time point).

DISCUSSION

The main findings of this study were that CIP induced an increase in ICAM-1 mRNA and protein expression at the BBB and that systemic proinflammatory mediators played no apparent role in the early disruption of the BBB (1–6 h) observed in previous studies; however, brain region-specific increases in microglial activation suggest a potential for a central-mediated response. Results show that CIP induced a biphasic response in ICAM-1 protein expression and suggest that changes in BBB function and structure at the early and delayed phase may be due to different pathophysiological processes. The results also indicate an early BBB response with ICAM-1 mRNA detectable at 15 min postinjection and increased ICAM-1 protein expression by 3 h, which is in agreement with previous studies

Table 1. *Blood cell differential during CIP*

	SD		Time, h			
	Value	Range	0	3	48	72
RBC	6.9±0.6	6.1–7.9	7.0±0.9	6.7±0.5	6.7±0.5	7.2±0.4
WBC	4.8±1.4	2.4–7.0	4.0±1.1	3.9±1.2	5.5±1.1	5.8±1.7
Hct			40.0±4.7	37.9±3.3	40.4±1.9	40.8±2.2
Platelets			719±166	736±48	667±87	830±102
Lymphocytes			3.3±1.1	3.3±1.2	3.9±0.7	3.7±1.4
Undifferentiated			0.32±0.08	0.33±0.08	1.3±0.4*	1.1±0.4*
PMNs			0.43±0.12	0.32±0.08	0.6±0.3	0.7±0.2
% Lymphocytes	89.8±7.1	76–96	80.6±4.8	82.1±5.5	66.3±6.1*	65.6±7.5*
% Undifferentiated			8.2±2.2	8.8±1.8	23.0±7.0*	21.0±3.3*
% PMNs	9.7±6.6	4–23	11.3±3.8	9.1±4.2	10.7±5.7	13.4±5.3

Values are expressed as means ± SE (n = 6 per time point). SD values and ranges refer to "normal" ranges for blood chemistry as determined by Taconic. Undifferentiated refers to white blood cells (WBCs) that are too small or not able to be counted and definitively placed into one of the other categories. Results indicate that total WBC levels are not significantly different at any time point evaluated. In later time points (48 and 72 h), total lymphocyte counts do not change; however, percentage of lymphocytes significantly decreased, and percentage of "undifferentiated" cells (indeterminate banded, monocytes, undifferentiated) significantly increased in both number and percent of total percent WBC. *Significant difference compared with control ($P < 0.05$). CIP, λ-carrageenan-induced inflammatory pain; RBC, red blood cells; Hct, hematocrit; and PMNs, polymorphonuclear neutrophils.

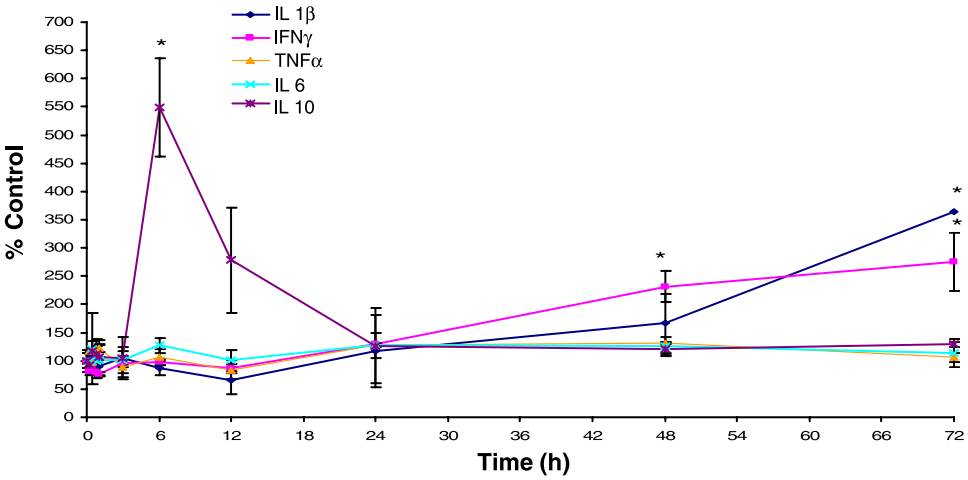

Fig. 6. Circulating levels of cytokines after CIP were determined by ELISA. No changes in circulating level of proinflammatory cytokines (TNF-α and IL-6) were observed during the 72-h time course. At 6 h, a fivefold increase in IL-10 was observed. At 48 h, a twofold increase in IFN-λ was observed and remained elevated out to 72 h. At 72 h, a threefold increase in IL-1β was seen. Each data point represents means ± SE (n = 6/time point). *Significant difference from control ($P < 0.05$).

showing increased ICAM-1 protein expression during the early stages of inflammation (14, 20).

To date, much of the research investigating ICAM-1 expression at the BBB has focused on interactions between leukocytes and endothelial cells to better understand the pathological processes of immune-mediated CNS diseases (26, 34, 42). However, because of the unique properties of the BBB (i.e., presence of tight junctions and lack of endocytotic activity), cerebral microvascular phenotype suggests an "epithelial-like" barrier; therefore, understanding the role of ICAM-1 at the BBB, especially during acute, regulatory changes in barrier function, may require a better understanding of how adhesion molecules function in epithelial tissues.

Results from this study suggest that during the early inflammatory phase (1–6 h), ICAM-1 was not involved in leukocyte transmigration, as shown by increased ICAM-1 immunostaining in the frontal and parietal cortex and thalamic regions of the brain at 3 h after CIP with no increase in neutrophil (MPO) immunoreactivity and the absence of surface expression of LFA-1 (CD18) on circulating PMNs. LFA-1 is a β_2-integrin that is necessary for high-affinity adhesion of circulating PMNs to ICAM-1. In this study, we found that ICAM-1 may play a more pronounced role in leukocyte transmigration during the delayed phase because increased ICAM-1 mRNA and protein expression was correlated with increased neutrophil (MPO) immunoreactivity and $CD18^{high}$ PMNs at 48 h. In addition, although total WBC did not increase over the 72 h, the increase in undifferentiated leukocytes suggests increased turnover of PMNs. Of particular interest is the close correlation between increased ICAM-1 expression (early and delayed phase) and

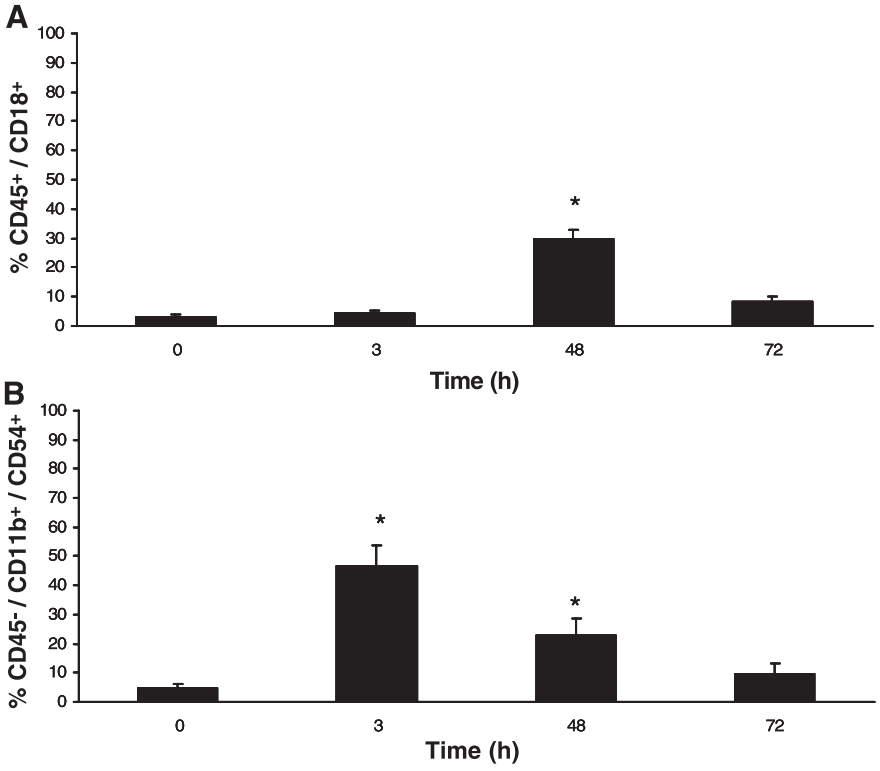

Fig. 7. Flow cytometric immunophenotyping of blood and microglial isolates after CIP. *A*: CD18 (lymphocyte function-associated antigen-1) expression on CD45-positive cells (leukocytes) in blood at 48 h compared with control (0 h) shows a significant increase ($P < 0.01$). *B*: CD54 (ICAM-1) expression in microglial isolates ($CD45^{low}$/CD11 b/c^{high}) at 3 and 48 h compared with control (0 h) shows a significant increase ($P < 0.01$). Each bar represents means ± SE. (n = 3/time point). *Significant difference from control ($P < 0.05$).

our previous observations regarding changes in BBB permeability and tight junction protein expression. Whereas no direct association between ICAM-1 and tight junction protein expression has been shown, several studies demonstrate a correlation between increased BBB permeability and neutrophil transmigration (1, 9).

On the basis of these investigations, it is becoming evident that the biphasic responses elicited by CIP at the BBB have different pathophysiological profiles. An understanding of the possible mechanisms and signaling pathways involved in these changes is a vital consideration in studies of BBB disruption during disease/injury. Several assays examined the systemic contribution to previously observed changes in BBB function and structure. Serum concentration of proinflammatory cytokines (IL-1β, IFN-γ, TNF-α, and IL-6) remained unchanged during the early phase (1–6 h) of CIP; however, a fivefold increase in IL-10 was observed at 6 h. IL-10 is an anti-inflammatory cytokine (11, 22) that inhibits release of proinflammatory cytokines and acts as a protective mechanism in a number of inflammatory disorders, including endotoxic and septic shock (33), acute respiratory distress syndromes (36), and CNS injury (7). The increased IL-10 serum concentration is most likely an indication of reparative properties within the paw and may play a role in the restoration of BBB permeability seen by 12 h after CIP. Interestingly, a twofold increase in IL-1β at 48 h after CIP that remained elevated out to 72 h and a threefold increase in IFN-γ at 72 h were observed. The increased circulating proinflammatory cytokines at 48–72 h, the increased number of $CD45^{high}/CD18^{high}$ PMNs, and changes in the WBC profile at 48 h suggest a secondary inflammatory action resulting in systemic effects on the BBB during the delayed phase.

One of the most intriguing observations of this study was the increased expression of activated microglia in the brain at 3 h after CIP. The early activation of microglia suggests that changes observed at the BBB after CIP have a central-mediated component. The mechanisms by which these changes occur and the ramifications of microglial activity after CIP are currently unresolved. However, a number of recent studies suggested that early microglial activation plays a neuroprotective role and that microglial activation was associated with increased ICAM-1 expression. Interestingly, brain region-specific changes in ICAM-1 expression and microglia occurred bilaterally, although sensory signaling through spinal tracts runs contralateral to the affected side. A recent novel study (44) using functional magnetic resonance imaging identified brain regions involved in the experience and anticipation of painful stimuli. The results showed that efferent pain transmission enters the midbrain contralateral to the affected side but that transmission through the thalamus and higher brain centers occurred bilaterally. Furthermore, the study (44) showed that different types of painful stimuli (shock versus heat) produce transmission pathways that have both discrete and overlapping areas of activity within the brain. Thus the findings in this study along with the findings of BBB perturbations noted in our previous work (16, 17, 18) suggest that painful stimuli not only elicit alterations in BBB function and structure but that these alterations may be localized and region specific. Future studies will need to expand the investigation to examine other cortical areas and the midbrain as well as identify differences in sensory transmission based on the pain model.

ACKNOWLEDGMENTS

We thank Cynthia Cunningham, Director of the West Virginia University Flow Cytometry Core Facility, for assistance with the immunophenotypy studies.

GRANTS

Research was funded by West Virginia Research (to J. D. Huber) and National Institutes of Health Grants NS-42652 (to T. P. Davis) and DA-11271 (to T. P. Davis).

REFERENCES

1. **Bolton SJ and Perry VH.** Differential blood-brain barrier breakdown and leucocyte recruitment following excitotoxic lesions in juvenile and adult rats. *Exp Neurol* 154: 231–240, 1998.
2. **Campanella M, Sciorati C, Tarozzo G, and Beltramo M.** Flow cytometric analysis of inflammatory cells in ischemic rat brain. *Stroke* 33: 586–592, 2002.
3. **Chauvet N, Palin K, Verrier D, Poole S, Dantzer R, and Lestage J.** Rat microglial cells secrete predominantly the precursor of interleukin-1beta in response to lipopolysaccharide. *Eur J Neurosci* 14: 609–617, 2001.
4. **Corti R, Hutter R, Badimon JJ, and Fuster V.** Evolving concepts in the triad of atherosclerosis, inflammation and thrombosis. *J Thromb Thrombolysis* 17: 35–44, 2004.
5. **Couraud PO.** Infiltration of inflammatory cells through brain endothelium. *Pathol Biol (Paris)* 46: 176–180, 1998.
6. **Danton GH and Dietrich WD.** Inflammatory mechanisms after ischemia and stroke. *J Neuropathol Exp Neurol* 62: 127–136, 2003.
7. **Dietrich WD, Chatzipanteli K, Vitarbo E, Wada K, and Kinoshita K.** The role of inflammatory processes in the pathophysiology and treatment of brain and spinal cord trauma. *Acta Neurochir Suppl (Wien)* 89: 69–74, 2004.
8. **Dinkel K, MacPherson A, and Sapolsky RM.** Novel glucocorticoid effects on acute inflammation in the CNS. *J Neurochem* 84: 705–716, 2003.
9. **Durieu-Trautmann O, Chaverot N, Cazaubon S, Strosberg AD, and Couraud PO.** Intercellular adhesion molecule 1 activation induces tyrosine phosphorylation of the cytoskeleton-associated protein cortactin in brain microvessel endothelial cells. *J Biol Chem* 269: 12536–12540, 1994.
10. **Farkas IG, Czigner A, Farkas E, Dobo E, Soos K, Penke B, Endresz V, and Mihaly A.** Beta-amyloid peptide-induced blood-brain barrier disruption facilitates T-cell entry into the rat brain. *Acta Histochem* 105: 115–125, 2003.
11. **Fiorentino DF, Zlotnik A, Mosmann TR, Howard M, and O'Garra A.** IL-10 inhibits cytokine production by activated macrophages. *J Immunol* 147: 3815–3822, 1991.
12. **Grossmann R, Stence N, Carr J, Fuller L, Waite M, and Dailey ME.** Juxtavascular microglia migrate along brain microvessels following activation during early postnatal development. *Glia* 37: 229–240, 2002.
13. **Guo LH, Trautmann K, and and Schluesener HJ.** Expression of P2X4 receptor by lesional activated microglia during formalin-induced inflammatory pain. *J Neuroimmunol* 163: 120–127, 2005.
14. **Hang CH, Shi JX, Tian J, Li JS, Wu W, and Yin HX.** Effect of systemic LPS injection on cortical NF-kappaB activity and inflammatory response following traumatic brain injury in rats. *Brain Res* 1026: 23–32, 2004.
15. **Harcourt BH, Sanchez A, and Offermann MK.** Ebola virus selectively inhibits responses to interferons, but not to interleukin-1beta, in endothelial cells. *J Virol* 73: 3491–3496, 1999.
16. **Hau VS, Huber JD, Campos CR, Davis RT, and Davis TP.** Effect of lambda-carrageenan-induced inflammatory pain on brain uptake of codeine and antinociception. *Brain Res* 1018: 257–264, 2004.
17. **Huber JD, Witt KA, Hom S, Egleton RD, Mark KS, and Davis TP.** Inflammatory pain alters blood-brain barrier permeability and tight junctional protein expression. *Am J Physiol Heart Circ Physiol* 280: H1241–H1248, 2001.
18. **Huber JD, Hau VS, Borg L, Campos CR, Egleton RD, and Davis TP.** Blood-brain barrier tight junctions are altered during a 72-h exposure to λ-carrageenan-induced inflammatory pain. *Am J Physiol Heart Circ Physiol* 283: H1531–H1537, 2002.
19. **Isogai N, Tanaka H, and Asamura S.** Thrombosis and altered expression of intercellular adhesion molecule-1 (ICAM-1) after avulsion injury in rat vessels. *J Hand Surg [Br]* 29: 230–234, 2004.

20. **Ito T, Kumamoto T, Horinouchi H, Yukishige K, Sugihara R, Fujimoto S, and Tsuda T.** Adhesion molecule expression in experimental myositis. *Muscle Nerve* 25: 409–418, 2002.
21. **Jaworowicz DJ, Korytko PJ, Singh-Lakhman S, and Boje KM.** Nitric oxide and prostaglandin E_2 formation parallels blood-brain barrier disruption in an experimental rat model of bacterial meningitis. *Brain Res Bull* 46: 541–546, 1998.
22. **Kasama T, Strieter RM, Lukacs NW, Burdick MD, and Kunkel SL.** Regulation of neutrophil-derived chemokine expression by IL-10. *J Immunol* 152: 3559–3569, 1994.
23. **Kim M, Carman CV, and Springer TA.** Bidirectional transmembrane signaling by cytoplasmic domain separation in integrins. *Science* 301: 1720–1725, 2003.
24. **Kyrkanides S, Moore AH, Olschowka JA, Daeschner JC, Williams JP, Hansen JT, and O'Banion MK.** Cyclooxygenase-2 modulates brain inflammation-related gene expression in central nervous system radiation injury. *Brain Res Mol Brain Res* 104: 159–169, 2002.
25. **Kyrkanides S, O'Banion MK, Whiteley PE, Daeschner JC, and Olschowka JA.** Enhanced glial activation and expression of specific CNS inflammation-related molecules in aged versus young rats following cortical stab injury. *J Neuroimmunol* 119: 269–277, 2001.
26. **Langford D and Masliah E.** Crosstalk between components of the blood brain barrier and cells of the CNS in microglial activation in AIDS. *Brain Pathol* 11: 306–312, 2001.
27. **Lassmann H, Zimprich F, Vass K, and Hickey WF.** Microglial cells are a component of the perivascular glia limitans. *J Neurosci Res* 28: 236–243, 1991.
28. **Lindia JA, McGowan E, Jochnowitz N, and Abbadie C.** Induction of CX3CL1 expression in astrocytes and CX3CR1 in microglia in the spinal cord of a rat model of neuropathic pain. *J Pain* 6: 434–438, 2005.
29. **Lub M, van Kooyk Y, van Vliet SJ, and Figdor CG.** Dual role of the actin cytoskeleton in regulating cell adhesion mediated by the integrin lymphocyte function-associated molecule-1. *Mol Biol Cell* 8: 341–351, 1997.
30. **Markovic-Plese S and McFarland HF.** Immunopathogenesis of the multiple sclerosis lesion. *Curr Neurol Neurosci Rep* 1: 257–262, 2001.
31. **Meagher L, Mahiouz D, Sugars K, Burrows N, Norris P, Yarwood H, Becker-Andre M, and Haskard DO.** Measurement of mRNA for E-selectin, VCAM-1 and ICAM-1 by reverse transcription and the polymerase chain reaction. *J Immunol Methods* 175: 237–246, 1994.
32. **Merodio M, Irache JM, Eclancher F, Mirshahi M, and Villarroya H.** Distribution of albumin nanoparticles in animals induced with the experimental allergic encephalomyelitis. *J Drug Target* 8: 289–303, 2000.
33. **Monneret G, Finck ME, Venet F, Debard AL, Bohe J, Bienvenu J, and Lepape A.** The anti-inflammatory response dominates after septic shock: association of low monocyte HLA-DR expression and high interleukin-10 concentration. *Immunol Lett* 95: 193–198, 2004.
34. **Paul R, Koedel U, Winkler F, Kieseier BC, Fontana A, Kopf M, Hartung HP, and Pfister HW.** Lack of IL-6 augments inflammatory response but decreases vascular permeability in bacterial meningitis. *Brain* 126: 1873–1882, 2003.
35. **Paxinos G and Watson C.** *The Rat Brain in Stereotaxic Coordinates* (4th ed.). New York: Elsevier, 2004, plate 29.
36. **Pease JE and Sabroe I.** The role of interleukin-8 and its receptors in inflammatory lung disease: implications for therapy. *Am J Respir Med* 1: 19–25, 2002.
37. **Proescholdt MA, Jacobson S, Tresser N, Oldfield EH, and Merrill MJ.** Vascular endothelial growth factor is expressed in multiple sclerosis plaques and can induce inflammatory lesions in experimental allergic encephalomyelitis rats. *J Neuropathol Exp Neurol* 61: 914–925, 2002.
38. **Pu H, Tian J, Flora G, Lee YW, Nath A, Hennig B, and Toborek M.** HIV-1 Tat protein upregulates inflammatory mediators and induces monocyte invasion into the brain. *Mol Cell Neurosci* 24: 224–237, 2003.
39. **Pyo CW, Hur SS, Kim YK, Choi HB, Hong YS, Kim DW, Kim CC, Kim HK, and Kim TG.** Polymorphisms of IL-1B, IL-1RN, IL-2, IL-4, IL-6, IL-10, and IFN-gamma genes in the Korean population. *Hum Immunol* 64: 979–989, 2003.
40. **Sanz MJ, Nabah YN, Cerda-Nicolas M, O'Connor JE, Issekutz AC, Cortijo J, and Morcillo EJ.** Erythromycin exerts in vivo anti-inflammatory activity downregulating cell adhesion molecule expression. *Br J Pharmacol* 144: 190–201, 2005.
41. **Springer TA.** Traffic signals for lymphocyte recirculation and leukocyte emigration: the multistep paradigm. *Cell* 76: 301–314, 1994.
42. **Stanimirovic D and Satoh K.** Inflammatory mediators of cerebral endothelium: a role in ischemic brain inflammation. *Brain Pathol* 10: 113–126, 2000.
43. **Toborek M, Lee YW, Pu H, Malecki A, Flora G, Garrido R, Hennig B, Bauer HC, and Nath A.** HIV-Tat protein induces oxidative and inflammatory pathways in brain endothelium. *J Neurochem* 84: 169–179, 2003.
44. **Wager TD, Rilling JK, Smith EE, Sokolik A, Casey KL, Davidson RJ, Kosslyn SM, Rose RM, and Cohen JD.** Placebo-induced changes in fMRI in the anticipation and experience of pain. *Science* 303: 1162–1167, 2004.
45. **Wertheimer SJ, Myers CL, Wallace RW, and Parks TP.** Intercellular adhesion molecule-1 gene expression in human endothelial cells. Differential regulation by tumor necrosis factor-alpha and phorbol myristate acetate. *J Biol Chem* 267: 12030–12035, 1992.
46. **Yokomori H, Oda M, and Ishii H.** Improvement of overexpression of endothelin B receptor in human cirrhotic liver by interferon therapy. *J Gastroenterol* 38: 707–709, 2003.
47. **Zameer A and Hoffman SA.** Increased ICAM-1 and VCAM-1 expression in the brains of autoimmune mice. *J Neuroimmunol* 142: 67–74, 2003.